Journal of Colloid and Interface Science 571 (2020) 267–274

Contents lists available at ScienceDirect

Journal of Colloid and Interface Science

journal homepage: www.elsevier.com/locate/jcis

Scattering from colloidal cubic silica shells: Part II, static structure factors and osmotic equation of state

F. Dekker [a], B.W.M. Kuipers [a], Á. González García [a,b], R. Tuinier [a,b], A.P. Philipse [a,*]

[a] Van't Hoff Laboratory for Physical and Colloid Chemistry, Debye Institute for Nanomaterials Science, Padulaan 8, 3584 CH, Utrecht University, the Netherlands
[b] Laboratory of Physical Chemistry, Department of Chemical Engineering and Chemistry & Institute for Complex Molecular Systems, Eindhoven University of Technology, P.O. Box 513, 5600 MB, Eindhoven, the Netherlands

HIGHLIGHTS

- Scattering study on concentrated dispersions of cubic silica shells (CSS).
- First static structure factor of stable fluid of CSS.
- Osmotic compressibility of CSS can be described by Carnahan-Starling like equation of state.
- CSS in DMF with LiCl have effective hard-particle interactions.

GRAPHICAL ABSTRACT

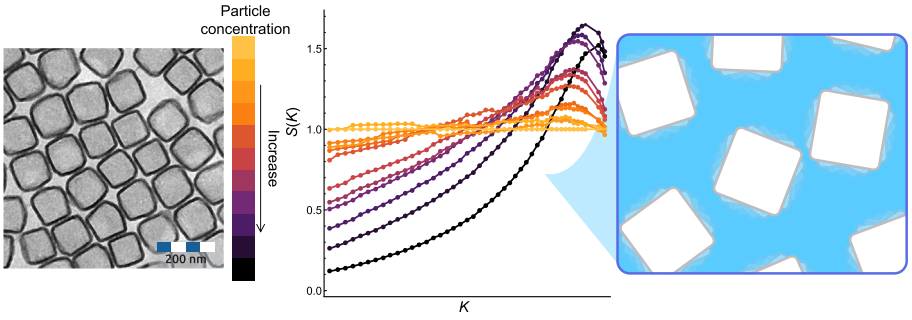

ARTICLE INFO

Article history:
Received 31 October 2019
Revised 13 February 2020
Accepted 15 February 2020
Available online 29 February 2020

Keywords:
Static light scattering
Colloidal cubic shells
Static structure factor
Superballs
Osmotic equation of state

ABSTRACT

Hypothesis: The shape of colloidal particles affects the structure of colloidal dispersions. The effect of the cube shape on the thermodynamics of colloidal cube dispersions has not yet been studied experimentally. Static light scattering measurements on colloidal cubic silica shells at finite concentrations allows us to measure the structure factor of colloidal cube fluids and to test theoretical predictions for the equation of state of hard convex superballs.

Experiments: Hollow silica nanocubes of varying concentrations in N,N,-dimethylformamide were studied with static light scattering. The structure factor was extracted from the scattering curves using experimental form factors. From this experimental structure factor, the specific density of the particles, and the osmotic compressibility were obtained. This osmotic compressibility was then compared to a theoretical equation of state of hard superballs.

Findings: The first experimental structure factors of a stable cube fluid are presented. The osmotic compressibility of the cube fluid can be described by the equation of state of a hard superball fluid, showing that silica cubes in N,N,-dimethylformamide with LiCl effectively interact as hard particles.

1. Introduction

Colloidal shape affects colloidal phase behaviour; both simulations [1] and experiments [2–4] show that various (liquid) crystal phases form for particles with different shapes. Dispersions of cubic particles exhibit rich phase behaviour upon assembly by depletion [5] or gravitational [6] forces. Further, it was found that the formed structures depend on the shape details of the cubes [2,5–7]. While the crystalline phase behaviour of cubic particles has been studied [2,6], no scattering studies have yet been conducted on the structure of colloidal cubes in the fluid phase. In this

* Corresponding author.
E-mail address: A.P.Philipse@uu.nl (A.P. Philipse).

https://doi.org/10.1016/j.jcis.2020.02.058
0021-9797/

paper we will focus on the concentration-dependent thermodynamic properties of colloidal cubic silica shells (CSS).

Understanding the interactions and stability of cubic particles is not only of fundamental interest, but is also important for potential applications of cubes in the area of sensing [8], catalysis [9] and energy storage [10] technologies. Additionally, cubic silica shells might find application in optical thin films [11,12], the preparation of which require knowledge and control of the stability of and interactions between the particles [13,14].

Static light scattering (SLS) is a well-established method for studying colloidal interactions [15], and has been used extensively to examine interactions between colloidal spheres. For example, the repulsions between hard and charged spheres [16,17] and depletion-mediated interactions [18] between colloidal spheres have been investigated by SLS. Additionally, SLS has been used to successfully study dispersions of anisotropic disk- [19] and rod-like [20] particles. This shows that SLS may also be a suitable technique to study the structural properties of dispersions of cubes with varying interactions. Such studies are wanted because even the concentration-dependent structure factor of cubic colloids interacting via a hard-particle potential, is yet unknown.

Cubic particles have been examined with scattering techniques such as small angle X-ray scattering [2,6], but no experimental reports are available on light scattering by concentrated fluids of cubic colloids in the Rayleigh-Gans-Debye regime. The lack of SLS studies on colloidal cubes might be due to absence of cubes that are suitable for that purpose. Until recently, reported cubic colloids were either too large [21,22] or made from light-absorbing materials like metals or metal-salts [23–25], factors which obstruct light scattering studies. Recently, we developed a method to prepare hollow silica nanocubes in the 80–150 nm range [26]. In Part I of this work on the scattering by cubic silica shells, we determined the particle form factor and particle refractive index [27]. Here we present scattering experiments on dispersions with cube volume fractions in the range 1–25 vol%. Experimental static structure factors of stable cube fluids are obtained, and the osmotic compressibility of colloidal cubes is compared to the equation of state of a hard superball fluid [28].

2. Theory

2.1. Static light scattering

In the Rayleigh-Gans-Debye regime, the excess scattering intensity of a collection of monodisperse spherical particles over that of the solvent can be written in terms of the Rayleigh ratio $R(K)$ as [27]

$$R(K) = P(K)S(K)v_c^2\rho(n_c - n_s)^2 2\pi^2 n_m^2 \lambda_0^{-4}, \tag{1}$$

with:

$$K = \frac{4\pi n_m}{\lambda_0}\sin\left(\frac{\theta}{2}\right). \tag{2}$$

Here, $P(K)$ is the form factor, $S(K)$ is the structure factor, v_c is the volume of the particles, ρ the number density of the particles, λ_0 the wavelength of light in vacuum, θ the scattering angle, and n_c, n_s, and n_m, the refractive indices of the particle, the solvent and the colloidal dispersion, respectively.

For a collection of discrete scatterers, the ensemble average intensity (without pre-factors) is given by [29]:

$$\langle I(K)\rangle = \sum_{j=1}^{N}\sum_{k=1}^{N}\langle F_j(K)F_k^*(K)e^{iK(r_j-r_k)}\rangle, \tag{3}$$

where $F_j(K)$ and $F_k(K)$ are the scattering amplitudes of particles j and k, and r_j and r_k are the locations of particles j and k respectively. Fore an ensemble of monodisperse spheres, Eq. (3) reduces to Eq. (1) with the structure factor $S(K)$, defined as [30,29]:

$$S(K) = \frac{1}{N}\sum_{j=1}^{N}\sum_{k=1}^{N}e^{iK(r_j-r_k)}, \tag{4}$$

where N is the total number of particles. In the case of cubic silica shells, the simplification of Eq. (3) to Eqs. (1) and (4) only holds over the full K-range if orientational correlations are absent, or in the K regime where the scattering amplitudes are similar to the orientationally averaged scattering. No theory seems to be available to account for the orientational correlation in the scattering of concentrated cubic particles. However, calculated values of $F(K)$ for perfect cubic shells depicted in Fig. A.6, show that for $KR_{el} < 5$, the scattering amplitudes are similar for all particle orientations. This is in line with the scattering of rods that Dhont discusses [31], where it is shown that for low contrast and in the limit of low K the scattering equations of rods reduces to those of spheres. Additionally, Meijer *et al.* [6] demonstrated that the crystal structure of superball particles with $m = 3.6$ in the crystal phase, where orientational correlation between the particles is present, can be resolved by considering the particles as monodisperse spheres. In light of the arguments presented above, we think the static light scattering of cubic silica shells can be initially analysed in terms of equations for monodisperse spheres, especially in the low K regime, in which we operate.

Eq. (4) describes how correlations between particle positions, influence the scattering intensity. For concentrated fluids of hard spheres, the structure factor can be approximated and calculated over the full K-range by the Percus–Yevick model [32]. For our cubic silica shells, no comparison with theory can yet be made over the full K-range of our experiments. At zero wavevector, however, the structure factor couples directly to the thermodynamic properties of a particle fluid via the general relation [33]:

$$\frac{1}{S(K=0)} = \frac{1}{k_B T}\left(\frac{\partial\Pi}{\partial\rho}\right)_T. \tag{5}$$

Here k_B is the Boltzmann's constant, T the absolute temperature in Kelvin, ρ is the particle number density and Π the osmotic pressure. $S(K=0)$ is directly coupled to the osmotic compressibility and $K \to 0$ is therefore often referred to as the thermodynamic limit. The osmotic compressibility, in turn, follows from the equation of state for a fluid of hard particles [34]. Recently, we developed a way to calculate the equation of state for superball particles with an arbitrary shape parameter m [28], which we will use here to link theory to our experiments.

2.2. Superballs

Superballs are mathematical shapes in the form of cubic particles with rounded edges. The superball shape is defined by [35]:

$$\left|2\frac{x}{R_{el}}\right|^m + \left|2\frac{y}{R_{el}}\right|^m + \left|2\frac{z}{R_{el}}\right|^m = 1 \tag{6}$$

where m is the shape parameter and R_{el} is the edge length of the superball. For $m = 2$ and $m = \infty$, Eq. (6) describes a perfect sphere and a cube, respectively. The equation of state for hard superballs is [28]:

$$\frac{\Pi v_c}{k_B T} = \frac{\phi + \mathfrak{Q}\phi^2 + \mathfrak{R}\phi^3 - \mathfrak{S}\phi^4}{(1-\phi)^3}. \tag{7}$$

Here, ϕ is the volume fractions of superballs, and:

$$\mathfrak{Q} = 3\gamma - 2,\ \mathfrak{R} = 1 - 3\gamma(1-\gamma),\ \mathfrak{S} = \gamma(6\gamma - 5), \tag{8}$$

where the parameter γ is defined by [36]:

$$\gamma = \frac{s_c c_c}{3 v_c}. \tag{9}$$

Here s_c, c_c and v_c are the surface area, the surface integrated mean curvature [37] and the volume of the particle, respectively. The asphericity parameter γ measures the extent to which a convex particle deviates from a spherical shape and is related to m. For low volume fractions we obtain from Eq. (7)

$$\frac{\Pi v_c}{k_B T} = \phi + B_2\phi^2 + \ldots. \tag{10}$$

Here, B_2 is the second osmotic virial coefficient normalised by the colloid particle volume, and can be obtained from γ via:

$$B_2 = 3\gamma + 1. \tag{11}$$

For spheres (m = 2), $B_2 = 4$ and for perfect cubes ($m = \infty$), B_2 = 5.5. For spheres, (γ = 1), Eq. (7) reduces to the Carnahan-Starling equation of state for hard spheres. In the equation of state [Eq. (7)], the osmotic pressure is given as a function of particle volume fraction. Generally, the volume fraction is not precisely known; the experimental concentration measure is colloid weight per dispersion volume. Scaled particle theory predicts that $\ln[S(K=0)^{-1}]$ increases linearly with ϕ up to ϕ = 0.4 [15], which allows us to determine the specific volume of the particles (σ), for the conversion of weight concentration to volume fractions, a procedure proposed by de Kruif *et al.* [30].

3. Materials and methods

3.1. Materials

N,N-Dimethylformamide (DMF, Anhydrous 99.8%) was purchased from Sigma–Aldrich and LiCl (Anhydrous, 99%) was obtained from Alfa Aesar. Particles were concentrated in DMF with 40 mM LiCl. For DMF, this results in a Debye screening length in the order of κ^{-1} = 1 nm.

4. Preparation of cubic silica shells

Cubic silica shells were prepared by using a template of cubic Cu_2O nanoparticles with an edge length R_{el} of 105 ± 11 nm. These particles were coated with a silica shell using the PVP assisted Stöber method [21,38]. After dissolving the core in nitric acid, cubis silica shells were obtained with an R_{el} of 125 ± 10 nm. Experimental details are presented in previous work [26]. A TEM micrograph of the particles used in this study is presented in Fig. 1.

4.1. Static light scattering

For the analysis of particles with SLS, a home-built setup was used, schematically depicted in Fig. A.1. In the set-up a mercury lamp is used as a light source. The light passes several optical filters to control the intensity, wavelength, polarisation and beam width/height. The scattered light is collected by a movable detector that scans over a scattering angle range $20° \leqslant \theta \leqslant 140°$. The samples were prepared by redispersing the particles in DMF filtered with 0.2 μm PTFE filters and transferring the dispersion to a dust-free cuvette. The cuvette was subsequently placed in a toluene bath to perform the experiment.

4.2. Structure factor measurements

Scattering curves of the most concentrated sample (Table A.1) were measured for light with wavelengths λ = 365 nm and 404 nm. The sample was then diluted, after which a new set of scattering curves was measured. This dilution procedure was repeated until the scattering intensity was too low to obtain reliable scattering curves. The concentration of the sample with the lowest concentration was then determined by drying a known volume, weighing the solid residue and correcting for LiCl present in the sample. Dilution factors and concentrations are listed in Table A.1.

5. Results

5.1. Measured scattering curves

In Fig. 2 static light scattering curves from cubic silica shells are plotted logarithmically against K^2 to obtain Guinier plots. It is seen that at low concentration, the curves are linear over almost the entire K range; only in the limit of low scattering angles and for high scattering angles, some deviations from linearity are visible. At low K these deviations are probably caused by residual dust particles or small clusters. For large K, especially at the lowest concentrations, the curves seem to bend upward. This upward swing in the scattering curve manifests the first minimum of the form factor, expected from theory to be located within the range $4 \cdot 10^7\ \mathrm{m}^{-1} < K < 5 \cdot 10^7\ \mathrm{m}^{-1}$ for hollow cubes with an R_{el} of 125 nm [27].

The slope of the Guinier plot was determined to extract the radius of gyration (R_g) of the particles and to extrapolate the scattered intensity in the limit $K \to 0$. For the lowest concentrations, obtained radii of gyration are R_g = 75.7 ± 0.4 nm and 75.76 ± 0.24 nm for λ = 365 nm and 404 nm, respectively. These values agree with the R_g calculated from TEM data (75 ± 6 nm). The slight increase in radius of gyration determined by SLS with respect to TEM is expected, since larger particles scatter more light than smaller particles do. This results in a larger apparent size from SLS. Scattering of spheres in the Guinier region, for instance yields an average radius R_m from $R_m^2 = \langle R^8\rangle/\langle R^6\rangle$, which differs from the size determined from TEM analysis, yielding a number average $\langle R\rangle$ [39]. We expect that the scattering results of cubic silica shells manifest a similar, higher order moment of the size distribution. The extrapolated scattering intensity from SLS at $K = 0$ is plotted as a function of concentration in Fig. 3. Fluctuation theory and scaled particle theory predict [15,33] that the scattering intensity for K = 0 has a maximum around $\phi \approx 0.12$ for hard particles with γ = 1 (spheres). This maximum follows from the expression for $S(K=0)$ from scaled particle theory [15];

$$\frac{1}{k_B T}\left(\frac{\partial \Pi}{\partial \rho}\right) = \frac{[1+(3\gamma-1)\phi]^2}{(1-\phi)^4}, \tag{12}$$

which indicates that the structure factor suppresses the total scattering intensity for $K = 0$. Eq. (12) can also be derived directly from Eq. (7). Combining Eq. (12) with Eq. (1) and using that $P(K=0) = 1$ and $\phi = \rho v_c$ it follows that the scattering intensity increases linearly at low volume fractions but passes through a maximum around $\phi \approx 0.12$. In both plots in Fig. 3, the maximum is visible. Both maxima occur at a concentration of roughly 100 g/L, indicating that the maximum concentration of 220 g/L corresponds to a volume fraction of roughly 0.24. This results also provide an estimated specific volume of the particles of 1.2 mL/g.

5.2. Structure factor

The structure factor $S(K)$ can be extracted by dividing Rayleigh ratio's and correcting for the concentration:

$$S(K) = \frac{R(K,c)}{R(K,c_0)}\frac{c_0}{c}. \tag{13}$$

Here $R(K,c)$ is the Rayleigh ratio for concentration c and $R(K,c_0)$ is the Rayleigh ratio for the lowest concentration c_0. We expect $S(K)$

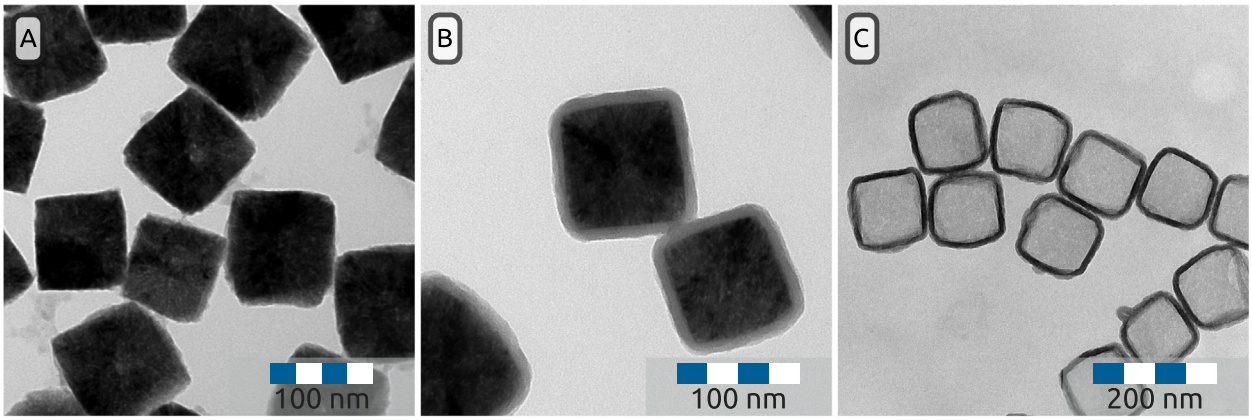

Fig. 1. TEM micrograph of the particles that were used for the scattering experiments. A: The cubic cuprous oxide template. B: The coated core shell particles. C: The cubic silica shells with an average edge length of 125 ± 10 nm and an *m* value of 4.1 ± 0.6.

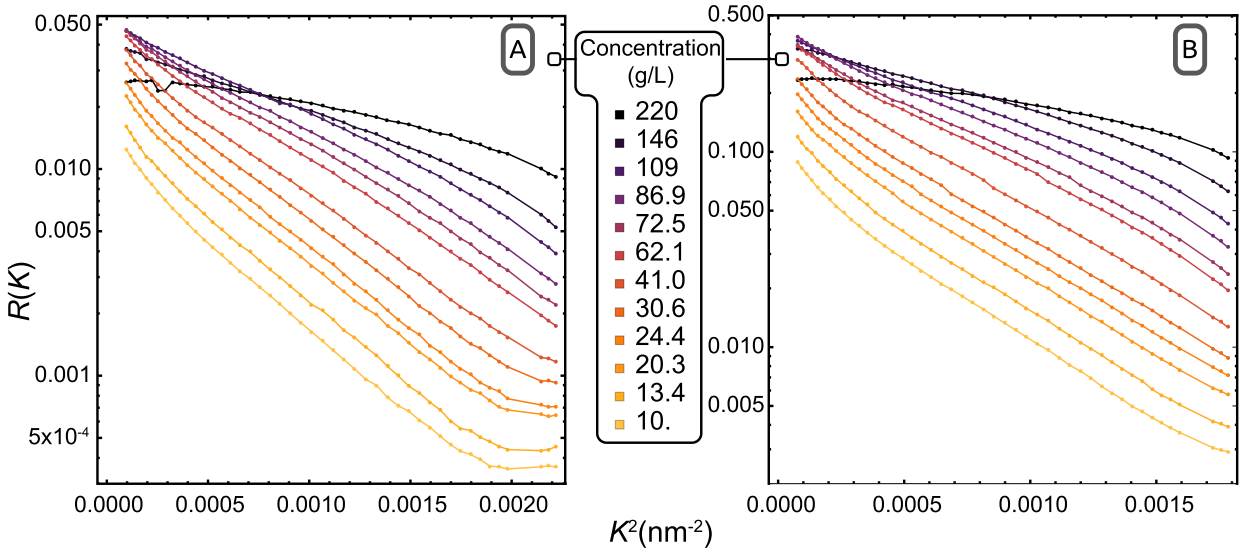

Fig. 2. Scattering curves for dispersions containing particles depicted in Fig. 1 in DMF with 40 mM LiCl. Particle concentrations range from 220 g/L to 10 g/L. A: scattering intensities obtained using light with λ = 365 nm. B: scattering intensities obtained using light with λ = 404 nm. The curves connecting the data-points are t.o guide the eye.

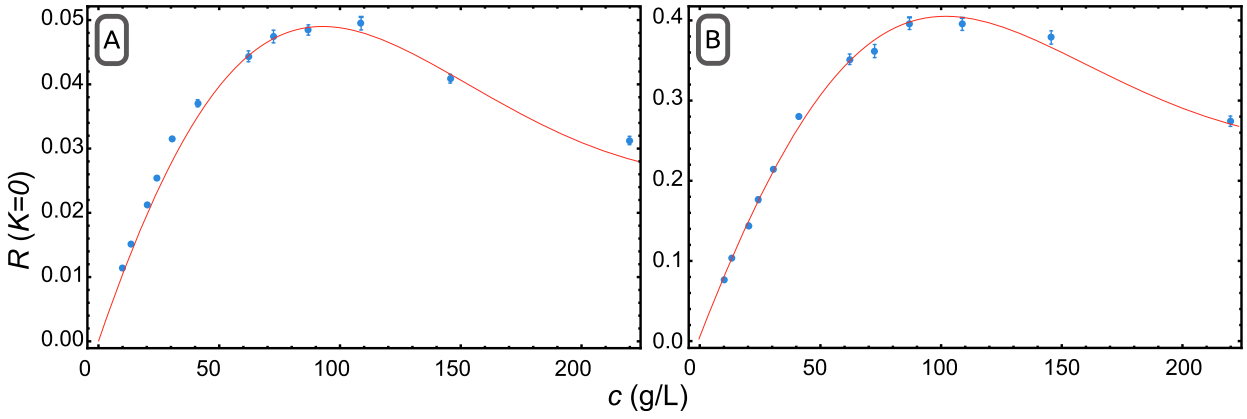

Fig. 3. Scattering intensity at $K = 0$, obtained by extrapolation. Left: Data obtained for light with λ = 365 nm. Right: Data obtained for light with λ = 404 nm. The solid curves are to guide the eye.

for $R(K, c_0)$ to be close to unity since the particle concentration is low [40]. From Fig. 4 it is clear that increasing the concentration results in a significant contribution of the structure factor to the overall scattering. The curves for concentrations of 13 and 20 g/L are close to 1 over almost the entire *K*-range, showing that it was justified to use the scattering profile for the lowest concentration

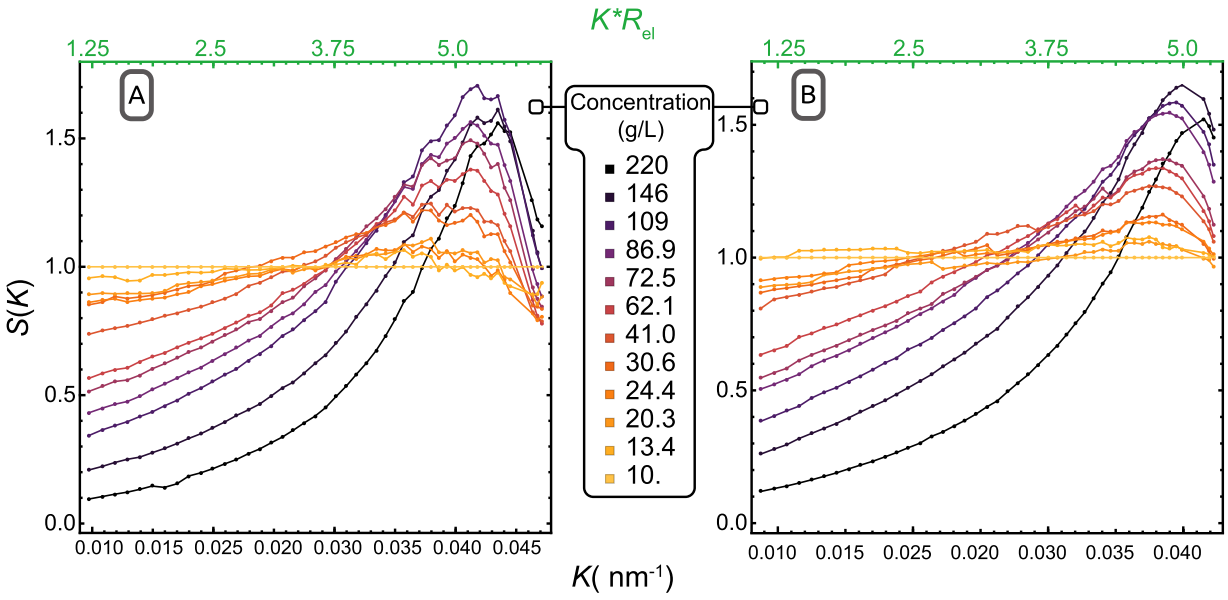

Fig. 4. Static structure factors measured with SLS as a function of scattering wave vector K. A: $S(K)$ for light with λ = 365 nm. B: $S(K)$ for light with λ = 404 nm. The curves connecting the data points are to guide the eye.

as the form factor. Hence, for low concentrations $S(K) \approx 1$. For high concentrations, $S(K \to 0)$ drops dramatically with increasing concentration and $S(K)$ exhibits a pronounced maximum for $KR_{el} \approx 5.4$. As discussed by Frenkel *et al.* [41] and de Kruif *et al.* [30], $\ln[S(K)]$ increases linearly with K^2 in the Guinier region, also for polydisperse particles, and so we can obtain the value of $S(K = 0)$ by linear extrapolation, as shown in Fig. A.2. The extrapolated values for $S(K = 0)$ can then be used to determine thermodynamic properties, as discussed in the Theory section. To determine the volume fraction of the silica cubes, theoretical values of $\ln[S(K = 0) - 1]$, obtained from Eq. (12) and Eq. (9) were plotted against ϕ for various m values (Fig. A.3, left). For superballs with an m value of 4, the slope is 8.06. This value is then used to determine the specific volume of the particles by plotting the experimental values for $\ln[S(K = 0)^{-1}]$ against the concentration (c) (Fig. A.3–2, right). It was found that the specific volume of the particles is 1.15 $\pm$ 0.18 mL/g, a value which corresponds well to the estimated specific volume (σ = 1.2 mL/g) from Fig. 3. Using σ volume fractions follow from: $\phi = c\sigma$ which enables us to compare our experiments to theory.

Since theoretical models for the structure factor of cubic particles seem to be absent yet, the experimental measured structure factors were compared to the Percus–Yevick (PY) results for the $S(K)$ for hard spheres [32,33]. In Fig. 5 the experimental structure

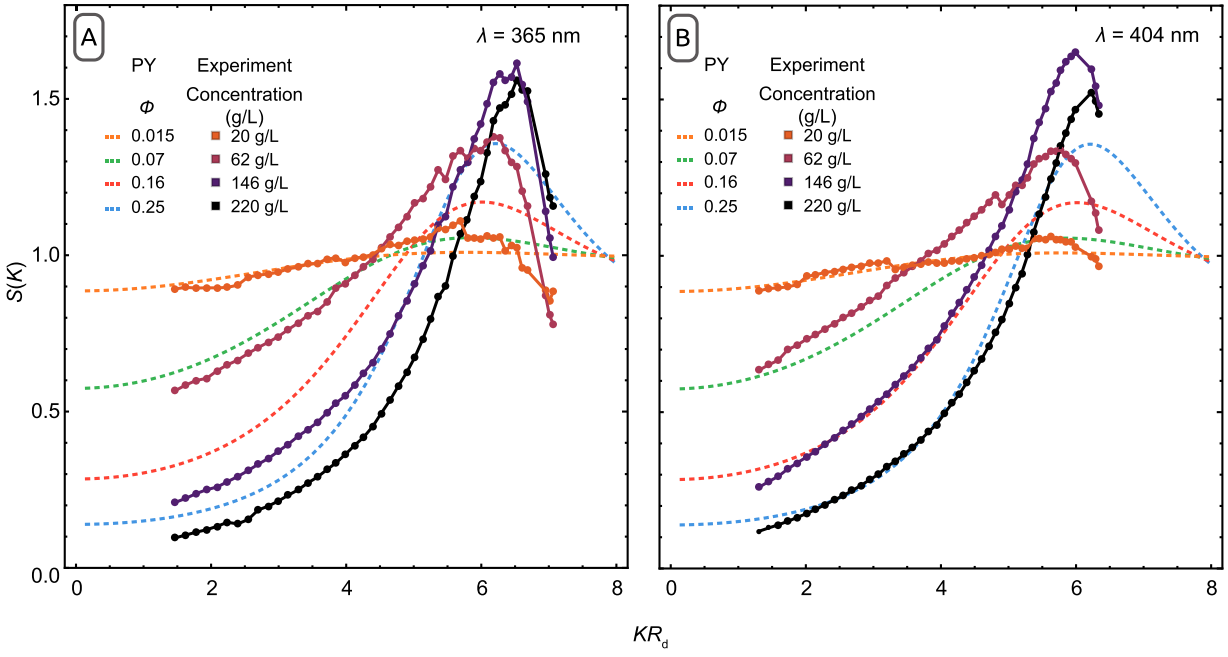

Fig. 5. Static structure factors measured with SLS compared with the Percus–Yevick approximation for hard spheres [32] as a function of scattering wave vector KR_d. A: $S(K)$ for light with λ = 365 nm. B: $S(K)$ for light with λ = 404 nm. The curves connecting the data points are to guide the eye.

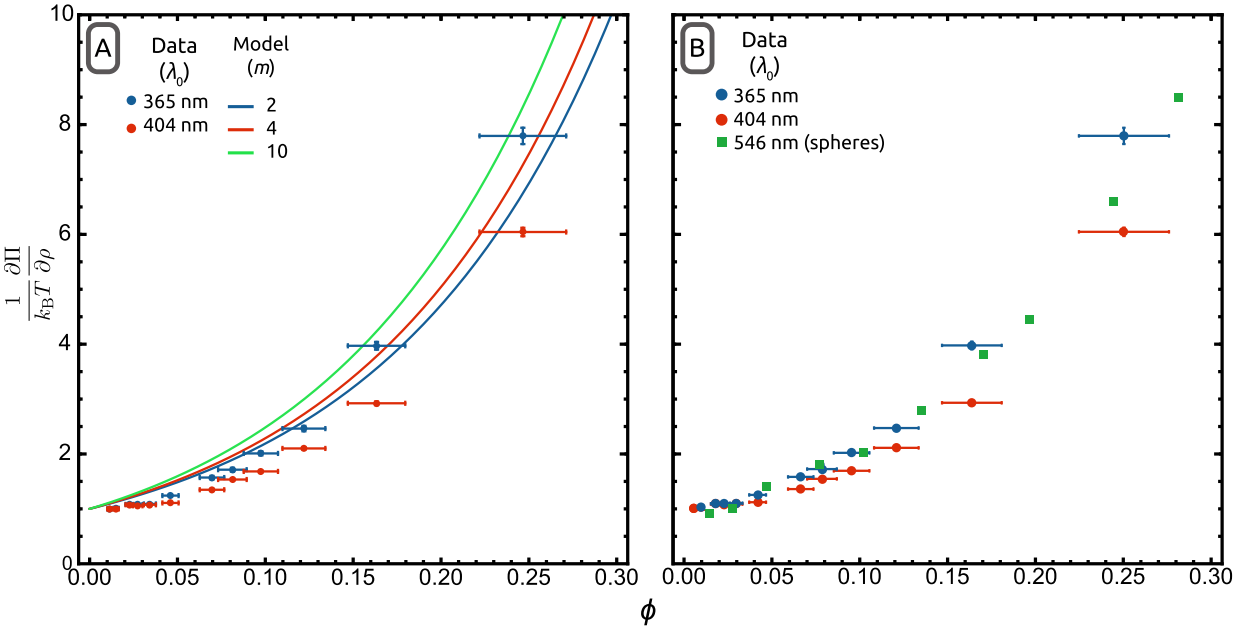

Fig. 6. Osmotic compressibility plotted against the particle volume fraction. The blue and red dots are experimental data obtained for light with λ = 365 and λ = 404 nm respectively. A: Obtained data compared to predictions for superballs with shape parameter m = 2, 4, and 10. B: Obtained data are compared to the osmotic equation of state of hard spheres from Ref. [42].

factor is plotted for four concentrations against KR_d, where R_d is the diagonal length of the cubic silica shells. The PY-approximation results for hard spheres are plotted for volume fractions corresponding to the calculated volume fractions, as depicted in Table A.1. In the figure it is visible that the experimental $S(KR_d)$ is described well by the PY-predictions for hard spheres, which are supposed to be accurate at least up to 30 vol% of hard spheres. The main difference is that at low K values ($KR_d < 2$) the structure factor of the cubic shells is lower compared to the hard sphere model, and that the first structure factor peak of the CSS around $KR_d \approx 6$ is significantly higher than the PY-predictions. This might be an effect of the cubic shape, but could also be an effect of a present double-layer repulsion, which promotes structure in the dispersion. Furthermore we note the PY-predictions only described the experimental structure factors well, when the data is normalised over the diagonal length of the cube R_d. When the data is normalised over the edge length of the cube R_{el}, the PY-model does not describe the data well, as depicted in Fig. A.4. This indicated that the cubic silica shells are free to rotate in de dispersion and the structure of the dispersion is mainly determined by the volume which freely rotating cubes explore.

In Fig. 6-A experimental values (data) of $S(K=0)^{-1}$ are plotted against theoretical predictions (curves) of the osmotic compressibility obtained from Eq. (5) using Eq. (7). Additionally in Fig. 6-B the obtained data are compared to the experimental osmotic compressibility as reported in Ref. [42], which is the only experimental equation of state of hard particles reported in literature that we are aware of. The two different experimental datasets are obtained by scattering of light with λ = 365 nm (blue dots) and 404 nm (red dots) and the theoretical curves are obtained from the equation of state of superballs with m = 2, 4, and 10. The uncertainty in $S(K=0)^{-1}$, represented by the vertical error bars, results from the error from the extrapolation of $S(K)$ to $K=0$. Considering the large difference in the values of $S(K=0)^{-1}$ between measurements done at λ = 365 nm and 404 nm, the actual error is probably significantly larger than the uncertainty obtained from extrapolation. The difference between the datasets is probably a result from the low scattering intensity at the lowest concentration, the method we used to extract $S(K)$ from the total scattering intensity $R(K)$, a difference in the relative refractive index [27], or a combination thereof. The uncertainty in the volume fraction of the particles (horizontal error bars) originates from the determination of the specific weight of the nanocubes (Fig. A.3-right) and is about 10%. The data clearly (semi-) quantitatively follow the same trend as the theoretical curves. At low and intermediate volume fractions, the experimental data are significantly lower compared to the theoretical predictions while at high volume fractions ($\phi > 0.15$) the experimental data follow the theoretical curves more closely. Besides the uncertainty in the experimental values of $S(K=0)^{-1}$ discussed above, another discrepancy arises from our method to determine the structure factor. To extract $S(K)$ using Eq. (13), scattering curves with a finite concentration is employed, while in Eq. (5) the scattering intensity in the limit of infinite dilution is used. This extraction method results in an off-set of the experimental osmotic compressibility with respect to the theoretical equation of state. If we correct for this in the theoretical equation of state, by shifting the curve so that $1/(S(K=0))=1$ at $\rho = 0.01$, the experimental data and theory are in good agreement over the entirely probed concentration range (Fig. A.5). The reasonable agreement of the experimental osmotic pressure with the theoretical equation of state implies that the pair-interactions between hollow silica cubes in DMF in 0.04 M LiCl can be described as the interactions between hard superballs.

6. Conclusions and outlook

The structure of dispersions of hollow silica nanocubes dispersed in N,N-dimethylformamide with LiCl, was studied employing static light scattering. The static structure factor was obtained as a function of concentration, resulting in the first experimental static structure factor of a stable cube fluid. From the structure factor in the thermodynamic limit we were able to determine the osmotic compressibility and the specific weight of the silica nanocubes. The experimental osmotic compressibility can be described

by a Carnahan–Starling like equation of state of hard superballs [28]. In the fluid phase, we find that the osmotic compressibility of cubic particles is similar to the osmotic compressibility of hard spheres [42], a similarity that is in agreement with scaled particle theory [15].

The results presented here allow us to further investigate the pair interactions between cubic colloids. Dispersions of cubic silica shells in N,N-dimethylformamide with LiCl are suited for experiments with dynamic light scattering. Since the wave vector regime of static light scattering is limited, extending the analysis to small angle X-ray and neutron scattering is required to further asses the effect that concentration has on the structure of cubic shell fluids. Neutron scattering in particular might increase our insight in the structure of these fluids since the contrast of the medium and the particles can be controlled. Additionally, static light scattering experiments can be extended to cubic shells with interactions beyond the hard-core potential. The silica particles in DMF are also promising for studying the influence of an added second compound, for instance non-adsorbing polymers, on the interaction between cubes in the fluid-phase [43].

CRediT authorship contribution statement

F. Dekker: Conceptualization, Methodology, Investigation, Writing - original draft, Visualization. **B.W.M. Kuipers:** Methodology, Validation, Writing - review & editing. **Á. González García:** Methodology, Validation, Writing - review & editing. **R. Tuinier:** Conceptualization, Writing - review & editing, Funding acquisition, Supervision. **A.P. Philipse:** Conceptualization, Writing - review & editing, Funding acquisition, Supervision.

Declaration of Competing Interest

The authors declare that they have no known competing financial interests or personal relationships that could have appeared to influence the work reported in this paper.

Acknowledgements

This project was funded by TTW under project number 14210. Dr. Leon Bremer, Dr. Damien Reardon, Dr. Filip Oosterlinck and Dr. Jurgen Scheerder (all DSM) from the Colloidal Mosaics project User Committee are thanked for helpful discussions. NWO-TTW is acknowledged for financial support. F.D. thanks Andrei Petukhov for helpful discussions. Á.G.G. thanks NWO-TA grant 731.015.025 for funding.

Appendix A. Supplementary material

Supplementary data associated with this article can be found, in the online version, at https://doi.org/10.1016/j.jcis.2020.02.058.

References

[1] P.F. Damasceno, M. Engel, S.C. Glotzer, Predictive self-assembly of polyhedra into complex structures, Science 337 (6093) (2012) 453–457, https://doi.org/10.1126/science.1220869.
[2] X. Zhang, Q. Di, F. Zhu, G. Sun, H. Zhang, Wideband anti-reflective micro/nano dual-scale structures: fabrication and optical properties, Micro & Nano Lett. 6 (11) (2011) 947, https://doi.org/10.1049/mnl.2011.0487.
[3] A. Kuijk, D.V. Byelov, A.V. Petukhov, A. Van Blaaderen, A. Imhof, Phase behavior of colloidal silica rods, Faraday Discuss. 159 (2012) 181–199, https://doi.org/10.1039/c2fd20084h.
[4] F.M. van der Kooij, M. Vogel, H.N.W. Lekkerkerker, Phase behavior of a mixture of platelike colloids and nonadsorbing polymer, Phys. Rev. E 62 (4) (2000) 5397–5402, https://doi.org/10.1103/PhysRevE.62.5397.
[5] L. Rossi, V. Soni, D.J. Ashton, D.J. Pine, A.P. Philipse, P.M. Chaikin, M. Dijkstra, S. Sacanna, W.T.M. Irvine, Shape-sensitive crystallization in colloidal superball fluids, Proc. Nat. Acad. Sci. USA 112 (17) (2015) 5286–5290, https://doi.org/10.1073/pnas.1415467112.
[6] J.M. Meijer, A. Pal, S. Ouhajji, H.N.W. Lekkerkerker, A.P. Philipse, A.V. Petukhov, Observation of solid-solid transitions in 3D crystals of colloidal superballs, Nature Commun. 8 (2017) 14352, https://doi.org/10.1038/ncomms14352.
[7] R.D. Batten, F.H. Stillinger, S. Torquato, Phase behavior of colloidal superballs: Shape interpolation from spheres to cubes, Phys. Rev. E 81 (6) (2010) 061105, https://doi.org/10.1103/PhysRevE.81.061105. arXiv:1005.0534.
[8] L.J. Sherry, S.H. Chang, G.C. Schatz, R.P. Van Duyne, B.J. Wiley, Y. Xia, Localized surface plasmon resonance spectroscopy of single silver nanocubes, Nano Lett. 5 (10) (2005) 2034–2038, https://doi.org/10.1021/nl0515753.
[9] C. Wang, H. Daimon, Y. Lee, J. Kim, S. Sun, Synthesis of monodisperse Pt nanocubes and their enhanced catalysis for oxygen reduction, J. Am. Chem. Soc. 129 (22) (2007) 6974–6975, https://doi.org/10.1021/ja070440r.
[10] J.C. Park, J. Kim, H. Kwon, H. Song, Gram-scale synthesis of Cu_2O nanocubes and subsequent oxidation to CuO hollow nanostructures for lithium-ion battery anode materials, Adv. Mater. 21 (7) (2009) 803–807, https://doi.org/10.1002/adma.200800596.
[11] H.K. Raut, V.A. Ganesh, A.S. Nair, S. Ramakrishna, Anti-reflective coatings: A critical, in-depth review, Energy Environ. Sci. 4 (10) (2011) 3779, https://doi.org/10.1039/c1ee01297e.
[12] P.H. Lissberger, Optical applications of dielectric thin films, Rep. Prog. Phys. 33 (1) (1970) 197–268, https://doi.org/10.1088/0034-4885/33/1/305.
[13] N. Vogel, M. Retsch, C.-A. Fustin, A. del Campo, U. Jonas, Advances in colloidal assembly: the design of structure and hierarchy in two and three dimensions, Chem. Rev. 115 (13) (2015) 6265–6311, https://doi.org/10.1021/cr400081d.
[14] V. Lotito, T. Zambelli, Approaches to self-assembly of colloidal monolayers: A guide for nanotechnologists, Adv. Colloid Interface Sci. 246 (April) (2017) 217–274, https://doi.org/10.1016/j.cis.2017.04.003.
[15] A. Vrij, J. Jansen, J.K. Dhont, C. Pathmamanoharan, H. Fijnaut, Light scattering of colloidal dispersions in non-polar solvents at finite concentrations, Faraday Discuss. Chem. Soc. 76 (1983) 19–35, https://doi.org/10.1039/dc9837600019.
[16] A.K. Van Helden, J.W. Jansen, A. Vrij, Preparation and characterization of spherical monodisperse silica dispersions in nonaqueous solvents, J. Colloid Interface Sci. 81 (2) (1981) 354–368, https://doi.org/10.1016/0021-9797(81)90417-3.
[17] A.P. Philipse, C. Smits, A. Vrij, A light scattering contrast variation study on nonaqueous suspensions of coated silica spheres, J. Colloid Interface Sci. 129 (2) (1989) 335–352, https://doi.org/10.1016/0021-9797(89)90447-5.
[18] I. Bodnár, J.K. Dhont, H.N.W. Lekkerkerker, Pretransitional phenomena of a colloid polymer mixture studied with static and dynamic light scattering, J. Phys. Chem. 100 (50) (1996) 19614–19619, https://doi.org/10.1021/jp962553v.
[19] S. Bhatia, J. Barker, A. Mourchid, Scattering of disklike particle suspensions: Evidence for repulsive interactions and large length scale structure from static light scattering and ultra-small-angle neutron scattering, Langmuir 19 (3) (2003) 532–535, https://doi.org/10.1021/la0265732.
[20] J. Buitenhuis, J.K.G. Dhont, H.N.W. Lekkerkerker, Static and dynamic light scattering by concentrated colloidal suspensions of polydisperse sterically stabilized boehmite rods, Macromolecules 27 (25) (1994) 7267–7277, https://doi.org/10.1021/ma00103a006.
[21] S.I. Castillo, S. Ouhajji, S. Fokker, B.H. Erné, C.T. Schneijdenberg, D.M. Thies-Weesie, A.P. Philipse, Silica cubes with tunable coating thickness and porosity: From hematite filled silica boxes to hollow silica bubbles, Microporous Mesoporous Mater. 195 (2014) 75–86, https://doi.org/10.1016/j.micromeso.2014.03.047.
[22] L. Rossi, S. Sacanna, W.T.M. Irvine, P.M. Chaikin, D.J. Pine, A.P. Philipse, Cubic crystals from cubic colloids, Soft Matter 7 (9) (2011) 4139–4142, https://doi.org/10.1039/C0SM01246G.
[23] Y. Sun, Y. Xia, Shape-controlled synthesis of gold and silver nanoparticles, Science 298 (5601) (2002) 2176–2179.
[24] L. Gou, C.J. Murphy, Solution-phase synthesis of Cu_2O nanocubes, Nano Lett. 3 (2) (2003) 231–234, https://doi.org/10.1021/nl0258776.
[25] D.H. Napper, R.H. Ottewil, Light scattering by cubic particles in the rayleigh-gans region, Kolloid-Zeitschrift und Zeitschrift für Polymere 192 (1964) 114–117.
[26] F. Dekker, R. Tuinier, A. Philipse, Synthesis of hollow silica nanocubes with tuneable size and shape, suitable for light scattering studies, Colloids Interfaces 2 (4) (2018) 44, https://doi.org/10.3390/colloids2040044.
[27] F. Dekker, B.W.M. Kuipers, A.V. Petukhov, R. Tuinier, A.P. Philipse, Scattering from colloidal cubic silica shells, Part I: Particle form factors and contrast variation, J. Colloid Interface Sci. 571 (2020) 419–428, https://doi.org/10.1016/j.jcis.2019.11.002.
[28] Á. González García, J. Opdam, R. Tuinier, Phase behaviour of colloidal superballs mixed with non-adsorbing polymers, Eur. Phys. J. E 41 (9) (2018) 110, https://doi.org/10.1140/epje/i2018-11719-3.
[29] P.N. Pusey, Introduction to scattering experiments, in: T. Zhemb, P. Lindner (Eds.), Neutrons, X-Rays and Light. Scattering Methods Applied to Soft Condensed Matter, 1st ed., no. April, North Holland, 2016, pp. 552 (Ch. 1).
[30] C.G. de Kruif, W.J. Briels, R.P. May, A. Vrij, Hard-sphere colloidal silica dispersion. the structure factor determined with SANS, Langmuir 4 (15) (1988) 668.

[31] J.K. Dhont, An Introduction to Dynamics of Colloids, Elsevier B.V, Amsterdam, 1996.
[32] J.K. Percus, G.J. Yevick, Analysis of classical statistical mechanics by means of collective coordinates, Phys. Rev. 110 (1) (1958) 1–13, https://doi.org/10.1103/PhysRev.110.1.
[33] A. Vrij, R. Tuinier, Concentrated colloidal dispersions, in: J. Lyklema (Ed.), Fundamentals of Interface and Colloids Science Volume IV Particulate Colloids, 1st ed., Elsevier B.V., Amsterdam, 2005, pp. 692. https://doi.org/10.1017/CBO9781107415324.004 (Ch. 5).
[34] A.K. Van Helden, A. Vrij, Contrast variation in light scattering: Silica spheres dispersed in apolar solvent mixtures, J. Colloid Interface Sci. 76 (2) (1980) 418–433, https://doi.org/10.1016/0021-9797(80)90383-5.
[35] Y. Jiao, F.H. Stillinger, S. Torquato, Optimal packings of superballs, Phys. Rev. E 79 (4) (2009) 41309, https://doi.org/10.1103/PhysRevE.79.041309.
[36] S.M. Oversteegen, R. Roth, General methods for free-volume theory, J. Chem. Phys. 122 (21) (2005) 214502, https://doi.org/10.1063/1.1908765.
[37] T. Boublík, Equation of state of hard convex body fluids, Mol. Phys. 42 (1) (1981) 209–216, https://doi.org/10.1080/00268978100100161.
[38] C. Graf, D.L. Vossen, A. Imhof, A. Van Blaaderen, A general method to coat colloidal particles with silica, Langmuir 19 (17) (2003) 6693–6700, https://doi.org/10.1021/la0347859.
[39] A.P. Philipse, A. Vrij, Polydispersity probed by light scattering of secondary particles in controlled growth experiments of silica spheres, J. Chem. Phys. 87 (10) (1987) 5634–5643, https://doi.org/10.1063/1.453536.
[40] A.P. Philipse, A. Vrij, Determination of static and dynamic interactions between monodisperse, charged silica spheres in an optically matching, organic solvent, J. Chem. Phys. 88 (10) (1988) 6459–6470, https://doi.org/10.1063/1.454432.
[41] D. Frenkel, R.J. Vos, C.G. De Kruif, A. Vrij, Structure factors of polydisperse systems of hard spheres: A comparison of Monte Carlo simulations and Percus-Yevick theory, J. Chem. Phys. 84 (8) (1986) 4625–4630, https://doi.org/10.1063/1.449987.
[42] A.K. Van Helden, A. Vrij, Static light scattering of concentrated silica dispersions in apolar solvents, J. Colloid Interface Sci. 78 (2) (1980) 312–329, https://doi.org/10.1016/0021-9797(80)90570-6.
[43] F. Dekker, PhD thesis, Utrecht University, 2020.